ELSEVIER

NeuroImage

www.elsevier.com/locate/ynimg
NeuroImage 23 (2004) S56–S68

Computational anatomy and neuropsychiatric disease: probabilistic assessment of variation and statistical inference of group difference, hemispheric asymmetry, and time-dependent change

John G. Csernansky,[a,b,*] Lei Wang,[a] Sarang C. Joshi,[c] J. Tilak Ratnanather,[d] and Michael I. Miller[d]

[a]*Department of Psychiatry, Washington University School of Medicine, St. Louis, MO 63110, United States*
[b]*Department of Anatomy and Neurobiology, Washington University School of Medicine, St. Louis, MO 63110, United States*
[c]*Department of Radiation Oncology, Biomedical Engineering and Computer Science, University of North Carolina at Chapel Hill, Chapel Hill, NC 27599, United States*
[d]*Center for Imaging Science, Johns Hopkins University, Baltimore, MD 21218, United States*

Available online 11 September 2004

Three components of computational anatomy (CA) are reviewed in this paper: (i) the computation of large-deformation maps, that is, for any given coordinate system representations of two anatomies, computing the diffeomorphic transformation from one to the other; (ii) the computation of empirical probability laws of anatomical variation between anatomies; and (iii) the construction of inferences regarding neuropsychiatric disease states. CA utilizes spatial–temporal vector field information obtained from large-deformation maps to assess anatomical variabilities and facilitate the detection and quantification of abnormalities of brain structure in subjects with neuropsychiatric disorders. Neuroanatomical structures are divided into two types: subcortical structures—gray matter (GM) volumes enclosed by a single surface—and cortical mantle structures—anatomically distinct portions of the cerebral cortical mantle layered between the white matter (WM) and cerebrospinal fluid (CSF). Because of fundamental differences in the geometry of these two types of structures, image-based large-deformation high-dimensional brain mapping (HDBM-LD) and large-deformation diffeomorphic metric matching (LDDMM) were developed for the study of subcortical structures and labeled cortical mantle distance mapping (LCMDM) was developed for the study of cortical mantle structures. Studies of neuropsychiatric disorders using CA usually require the testing of hypothesized group differences with relatively small numbers of subjects per group. Approaches that increase the power for testing such hypotheses include methods to quantify the shapes of individual structures, relationships between the shapes of related structures (e.g., asymmetry), and changes of shapes over time. Promising preliminary studies employing these approaches to studies of subjects with schizophrenia and very mild to mild Alzheimer's disease (AD) are presented.

Keywords: Computational anatomy; Neuropsychiatric disease; Neuropsychiatric disorders

Introduction

Computational anatomy (CA) is being increasingly used to characterize abnormalities of brain structure in individuals with neuropsychiatric disorders (Ashburner et al., 2003; Thompson et al., 1997). Early studies of disorders such as schizophrenia and Alzheimer's disease (AD) focused on the measurement of volume loss as a disease characteristic (Scheltens et al., 2002). However, volume loss may only be a reliable characteristic of those individuals that have more chronic or severe forms of neuropsychiatric disorders (Csernansky et al., 2002). To identify individuals that have early or very mild forms of neuropsychiatric disorders, or who are at genetic risk for developing neuropsychiatric disorders, tools capable of detecting subtle disturbances in the neuroanatomy are needed.

CA offers new approaches for quantifying neuroanatomical shapes as well as volumes (Grenander and Miller, 1998). Because neuroanatomical shapes may be influenced by patterns of neuroanatomical connections (Van Essen, 1997), metrics related to shape may be particularly sensitive to subtle disturbances in neuronal organization that occur during neurodevelopment and underlie some neuropsychiatric disorders (Miller et al., 2002). The search for neuroanatomical markers of neuropsychiatric disorders can also

* Corresponding author. Department of Psychiatry, Washington University School of Medicine, Campus Box 8134, 660 South Euclid Avenue, St. Louis, MO 63110. Fax: +1 314 747 2182.
E-mail address: jgc@conte.wustl.edu (J.G. Csernansky).
Available online on ScienceDirect (www.sciencedirect.com.)

1053-8119/$ - see front matter © 2004 Elsevier Inc. All rights reserved.
doi:10.1016/j.neuroimage.2004.07.025

take advantage of the asymmetry of the hemispheres of the brain. Nearly all paired neuroanatomical structures are asymmetric to some degree, the normative pattern of hemispheric asymmetries being formed during neurodevelopment. Thus, abnormalities of hemispheric asymmetries may be used to characterize neurodevelopmental disturbances associated with neuropsychiatric disorders. Finally, recent studies of normal neurodevelopment and aging using CA have begun to reveal normative lifetime patterns of neuroanatomical change (Good et al., 2001; Toga et al., 1996; Sowell et al., 2003). These studies establish an essential framework for studies of neuropsychiatric disorders where the pathology can be characterized by examining time-dependent deviations from normative patterns.

In this paper, we review the progress we have made in developing the tools of CA to derive spatial–temporal vector field information from large-deformation maps, to assess anatomical variabilities, and to characterize abnormalities of brain structure in subjects with neuropsychiatric disorders. We divided neuroanatomical structures into two types: subcortical structures—gray matter (GM) volumes enclosed by a single surface—and cortical mantle structures—anatomically distinct portions of the cerebral cortical mantle layered between the white matter (WM) and cerebrospinal fluid (CSF), and developed image-based large-deformation high-dimensional brain mapping (HDBM-LD) and large-deformation diffeomorphic metric matching (LDDMM) to study the former structures and labeled cortical mantle distance mapping (LCMDM) to study the latter. In this paper, we illustrate the power of these methods for characterizing neuroanatomical abnormalities in subjects with two neuropsychiatric disorders, schizophrenia and Alzheimer disease (AD). Examples are given where these disease states are detected by quantifying the shapes of neuroanatomical structures, relationships between the shapes of related structures (e.g., neuroanatomical asymmetries), and changes in neuroanatomical shapes over time (i.e., neurodegeneration).

Neuroanatomical abnormalities associated with neuropsychiatric disease

In our laboratory, we have focused on applying CA to the study of two neuropsychiatric disorders—schizophrenia and AD. To a surprising degree, neuroanatomical abnormalities of similar networks of structures have been implicated in these disorders. However, there is a fairly well developed understanding of the cellular basis of AD, while the cellular basis of schizophrenia remains largely unknown. The following sections offer a brief review of the current literature on neuroanatomical abnormalities in schizophrenia and AD.

Schizophrenia

Schizophrenia is thought to be caused by the interaction of genetic effects and environmental insults that disturbs neurodevelopment and leads to changes in the structure and function of a network of connected brain structures (Cannon et al., 2003). Prominent among these brain structures are the hippocampus and other structures of the temporal lobe, the thalamus, the cingulate gyrus, and prefrontal cortex (Wright et al., 2000).

Magnetic resonance (MR) imaging and manual segmentation methods have uncovered a variety of neuroanatomical abnormalities in subjects with schizophrenia, including volume reductions of temporal lobe structures (Suddath et al., 1989) and the hippocampus (see Nelson et al. (1998) for meta-analysis). However, the magnitude of these differences in neuroanatomical volumes is small (approximately 5–10%) and sometimes difficult to discern from normal variation in volume associated with height and gender. In some studies, volume losses of such structures have been more prominent on the left side of the brain (McCarley et al., 1993; Shenton et al., 1992). More recently, automated analyses of hippocampal shape using CA have demonstrated that abnormalities of hippocampal shape, localized to head of the hippocampus, accompany losses of hippocampal volume (Csernansky et al., 1998, 2002). Shenton et al. (1992) and McCarley et al. (1993) have also reported volume reductions of the parahippocampal gyrus and the superior temporal gyrus in individuals with schizophrenia.

Postmortem studies of individuals with schizophrenia have suggested possible cellular correlates of these volume and shape abnormalities; that is, decreases in the density and size of hippocampal pyramidal cells (Benes et al., 1991; Falkai and Bogerts, 1986; Jeste and Lohr, 1989). In one postmortem study, reduced gray matter volume of the parahippocampal gyrus was also reported (Altshuler et al., 1990). Disturbances of the functional activation of the same brain regions have also been observed during cognitive tasks that assess working and long-term memory (Barch et al., 2002).

MR studies have also demonstrated that individuals with schizophrenia have reductions in the volume of cortical gray matter (Andreasen et al., 1986; Zipursky et al., 1992). In postmortem studies of individuals with schizophrenia, Selemon et al. (1998, 2002) showed that the loss of neuropil is the likely basis for these gray matter volume decreases. A reduction in neuronal somal size has also been found in the prefrontal cortex, further suggesting that the number or organization of neuronal processes is diminished in schizophrenia (Rajkowska et al., 1998). Again, functional neuroimaging studies have demonstrated abnormal functional activation of the cortex in schizophrenia subjects, especially the dorsolateral prefrontal cortex during memory tasks (Barch et al., 2002).

Because of its numerous connections with cortical structures, the thalamus has become a prominent focus of neuroanatomical study in schizophrenia (Giguere and Goldman-Rakic, 1988; Romanski et al., 1997; Yeterian and Pandya, 1988). MR studies employing manual segmentation methods have shown that the overall volume of the thalamic complex is reduced in schizophrenia subjects (Andreasen, 1984; Buchsbaum et al., 1996; Gur et al., 1998). Using CA, we showed that the shape of the thalamus, in particular, the anterior and posterior extremes of the structure, was also deformed in schizophrenia subjects (Csernansky et al., 2004b). Again, postmortem studies of schizophrenia brains suggest that the cellular basis for these volume and shape abnormalities may be reductions in neuronal number within specific thalamic nuclei (i.e., anterior nucleus, mediodorsal nucleus, and pulvinar nuclei) (Byne et al., 2002; Manaye et al., 1997; Pakkenberg, 1990; Young et al., 2000).

Alzheimer's disease

AD is a progressive neurodegenerative disease of late life. Like schizophrenia, AD is characterized by neuroanatomical abnormalities of the medial temporal lobe and cerebral cortex (Arnold et al.,

1991). However, in AD, it is the progression of these neuroanatomical structures over time that may be most characteristic of the disease (Du et al., 2003; Fox et al., 2000; 2001). Amyloid plaques, neurofibrillary tangles, and neuronal degeneration form the cellular basis of neurodegeneration in AD (Arnold et al., 1991; Hyman et al., 1987). Because the hippocampus and other limbic structures play a critical role in declarative memory (Squire and Zola-Morgan, 1991), neurodegeneration within them is the likely basis for memory loss early during AD.

Substantial volume losses (approximately 20%) in the hippocampus and parahippocampal gyrus have been reported in individuals with early forms of AD, and the progression of such volume losses correlates with symptomatic worsening (Fox et al., 1996b; Jack et al., 1998; Mungas et al., 2002; Wang et al., 2003). In fact, progression of hippocampal volume loss over time has been suggested as a sensitive means of discriminating AD from normal aging and other neurodegenerative diseases (Fox et al., 1996a; Jack et al., 1998.

CA is being increasingly applied to the problem of identifying early forms of AD (Ashburner et al., 2003). Using CA, we have shown that hippocampal shape as well as volume can be used to discriminate subjects with very mild DAT from age-matched control subjects (Csernansky et al., 2000), and that ante-mortem hippocampal volumes correlated the severity of postmortem tangle density in the hippocampus (Csernansky et al., in press). Fox and Freeborough (1997), Fox et al. (1996a, 2001), and Freeborough and Fox (1998) have performed longitudinal studies of individuals with DAT using voxel compression mapping (VBM), and identified specific regions of the brain where time-dependent changes are prominent. Because of its sensitivity to time-dependent changes in neuroanatomical structure, VBM may reduce the sample size required to detect the effects of drug treatments on brain structure that aim to alter the rate of disease progression in DAT subjects (Fox et al., 2000). Recently, we compared patterns of time-dependent change in hippocampal shape and volume in subjects with very mild DAT and non-demented controls (Wang et al., 2003). Hippocampal shape change and the rate of volume loss provided complementary information for distinguishing between DAT subjects and controls.

Analytic approaches to subcortical structures vs. subregions of the cortical mantle

The emerging field of computational anatomy

Digital brain atlases have long been available for co-registration of images of differing modality and volumetric analyses of neuropsychiatric diseases (Evans et al., 1991; Greitz et al., 1991; Jansen et al., 1989). However, the characterization of subtle anatomical aberrations, such as those likely to occur in patients with schizophrenia or early forms of AD, requires the quantification of neuroanatomical variation within local substructures of the brain. Other investigators have enhanced the precision of lower dimensional algorithms for image registration by exploiting important geometric features such as neuroanatomical landmarks and contours (Bookstein, 1978; Bookstein and Green, 1992; Toga et al., 1991). However, local application throughout the substructures of the brain is an inherent feature of the high dimensional algorithms of CA. The following section reviews CA algorithms specifically designed for the analysis of specific types of brain substructures.

The main difficulty to be addressed in the analysis of human brain structure is that anatomical substructures form highly complex systems, with large variation among individuals being the rule. D'Arcy Thompson, in his influential treatise 'On Growth and Form' in 1917, had the vision of "the Method of Coordinates, on which is based the Theory of Transformations." In CA, Christensen et al. (1993), Grenander and Miller (1994, 1998), Joshi et al. (1997), and Miller et al. (1997) have championed the idea that neuroanatomical structures can be represented as a collection of coordinate systems: landmark points (0D), curves (1D), surfaces (2D), and subvolumes (3D); the strategy of generating diffeomorphic transformations of these coordinate systems is then employed to represent their variability across different individuals. Governed by Grenander's general pattern theory, the anatomies are represented as deformable templates, with the space of the anatomical images being the set of images generated by the group of diffeomorphic transformations acting on the template with associated probability laws describing how they occur and how they vary. The transformations are detailed enough so that a large family of shapes may be generated while maintaining the precise topology of the template. There are three principal components within this framework of CA: (i) the computation of large-deformation maps, that is, for any given coordinate system representations of two anatomies, to compute the diffeomorphic transformation from one to the other; (ii) the computation of empirical probability laws of anatomical variation between anatomies; and (iii) the construction of inferences regarding clinical categories.

We divide neuroanatomical structures into two main types; that is, subcortical structures and subregions of the cortical mantle. Subcortical structures, including the hippocampus, the amygdala, the thalamus, and the basal ganglia, can be conceptualized as structures being enclosed by a single surface. While this conceptualization represents an oversimplification (e.g., the hippocampus is in reality a folded piece of layered cortex and the thalamus and the amygdala are composed of complicated arrays of individual nuclei) at the level of resolution of the MR scans currently being acquired, much information can be gained about normal and abnormal processes by quantifying the shape of the idealized surfaces that enclose these structures. By subregions of the cortical mantle, we refer to the anatomically distinct portions of the cerebral cortical mantle that are layered between white matter and cerebrospinal fluid (CSF). Other investigators have parcellated the cerebral cortex in stereotaxic space (Andreasen et al., 1986; Fischl et al., 2002; Zipursky et al., 1992). However, its functionality may be better appreciated when considering it as an arrangement of connected cortical surfaces (Van Essen, 1997).

Quantitative analysis of subcortical structures

Our analysis of subcortical structures is based on Grenander's general pattern theory by representing the typical brain structures via templates and their variabilities via probabilistic transformations applied to the templates (Christensen et al., 1993, 1994, 1995; Joshi et al., 1995a,b; Miller et al., 1993). The transformations are diffeomorphisms constrained by laws of continuum mechanics while allowing all data points independent freedom to match, so that the geometric properties of neuroanatomical substructures are preserved (e.g., unbroken surfaces) and their details are main-

tained. We call this method "large-deformation high-dimensional brain mapping" (HDBM-LD). When the boundaries of template brain structures are carried along with the transformations, the volume and shape of the same brain structures in the target scans can be quantified.

HDBM-LD can also be used to quantify the asymmetries of paired subcortical structures. The intrasubject transformations from one side of the brain to the other (modulo identity) are examined, and variation away from zero becomes the measure of asymmetry (Wang et al., 2001). Finally, HDBM-LD can be used for quantifying changes in neuroanatomical shapes over time. For this purpose, the intrasubject transformations from the first to the second time point (modulo identity) are examined, and variation away from zero again becomes the measure of change (Wang et al., 2003).

Recently, "large-deformation diffeomorphic metric mapping" (LDDMM) has been developed by Beg et al. (2003b). LDDMM generates the geodesic map between shapes in the space of diffeomorphisms. Unlike the previous "greedy" procedure of HDBM-LD, which generates a particular (but not necessarily the shortest) path in the space of diffeomorphisms from the geodesic, the metric distance between anatomies represents a global optimization of the previously local in-time optimization of HDBM-LD. Using LDDMM, longitudinal neurodevelopmental and neurodegenerative processes associated with geodesic metrics can be computed by quantifying the geodesic connection between the corresponding elements in the template and target (Miller et al., 2002).

Quantitative analysis of subregions of the cortical mantle

The mantle of the cerebral cortex is a thin laminar structure (i.e., approximately 3 mm in thickness) with a large surface area. In recent years, cortical mantle reconstruction via statistical decision methods has been developed (Dale et al., 1999; Fischl et al., 2002; Joshi et al., 1999; Miller et al., 2000; Ratnanather et al., 2001; Shattuck et al., 2001; Sowell et al., 2000). Automated generation of the 2D surface coordinate system on the cortex has improved dramatically as well (Fischl et al., 2002; Hurdal et al., 1999; Shattuck et al., 2001; Thompson et al., 1996; Van Essen and Maunsell, 1980; Van Essen et al., 1998).

Over the last several years, we have developed new methods for the analysis of subregions of the cortical mantle. We first identify the 2D manifold surface associated with the gray matter/white matter (GM/WM) interface; each GM, WM, and CSF voxel is then labeled by its distance to this interface. Using this approach, the characteristics of specific regions of the cortical mantle can quantified via maps of frequency occurrence of the labeled voxels as functions of distance to GM/WM interface. We call this method "labeled cortical mantle distance mapping" (LCMDM) (Miller et al., 2003). These maps generated by LCMDM are sensitive to variabilities in the GM surface area, volume, and thickness that might be characteristic of neuropsychiatric diseases.

Statistical inferences on group differences

When trying to characterize the neuroanatomical abnormalities associated with a specific neuropsychiatric disorder, certain fundamental questions nearly always arise. First, and perhaps most importantly, one is asked to detect group differences in the structure of a particular brain region. This task, while seemingly straightforward, can be quite challenging when the data set is of very high dimensionality and the number of individuals in each group is small (i.e., approximately 20–50). As a correlate of the question of group difference, one can also ask whether the neuroanatomical relationships between two different structures or whether time-dependent patterns of change in a structure are altered. The analysis of the hemispheric asymmetry of a paired neuroanatomical structure can be considered as a special case of the former question. Below is a summary of our methodological approaches to the question of detecting group differences, and examples of applying these approaches to the study of schizophrenia and AD.

Methods for characterizing group differences of subcortical structures

To detect and quantify group difference in the structure of a subcortical structure, we first represent the template subcortical structure as a 2D smooth manifold $\mathbf{M}_0$, which is constructed as an enclosed triangulated surface at the external boundary that encloses its volume (Joshi et al., 1997). The diffeomorphic transformations h_i carry the template surface $\mathbf{M}_0$ into target anatomies, representing individual subcortical structures by the resulting surfaces $\mathbf{M}_i = h_i o \mathbf{M}_0$. Volumes of subcortical structures are then computed according to the Divergence Theorem of Gauss on the surface: $V_i = \frac{1}{3}\sum_{x \in \mathbf{M}_i} n_z v(x)$, where (x) is the surface element (i.e., face of a triangle) and n_z is the component of the unit surface normal vector in the perpendicular direction associated with each surface element. The average surface can then be defined by applying the average transformation $\bar{h} = \frac{1}{N}\sum_{i=1}^{N} h_i$ to the template surface: $\bar{\mathbf{M}} = \bar{h} o \mathbf{M}_0$. It follows that $\bar{\mathbf{M}}$ is a smooth manifold because h_i (hence $\bar{h}$) are diffeomorphisms (Boothby, 1986). Under a small-deformation assumption, $\bar{\mathbf{M}}$ is the minimum-energy representation of the population (Grenander and Miller, 1998).

Subcortical structure shape and probability measures of shape variation can then be characterized by Gaussian random fields indexed over the subcortical surface manifolds on which the transformation vectors are defined. Associated with the diffeomorphic transformations $\{h_i\}$ are a set of 3D Gaussian random vector fields modulo the identity map on the smooth subcortical manifold $U = \left\{u_i(x) = h_i(x) - x, x \in \bar{\mathbf{M}}\right\}$, which can be expanded using a complete orthonormal base $\{\lambda_k, \phi_k\}$ on the smooth manifold $\bar{\mathbf{M}}$ through the characteristic equation: $\lambda_k, \phi_k(x) = \int_{\bar{\mathbf{M}}} K(x,y)\phi_k(y)dv(y),\ x \in \bar{\mathbf{M}}$, where λ_k are the eigenvalues, ϕ_k are the eigenfunctions, and $dv(y)$ is the surface measure around the surface point y. Making the above integral equation discrete, the vector field covariance K can be expressed as $\hat{K}(x,y) = \frac{1}{N-1}\sum_{i=1}^{N} u_i(x)u_i^T(y)$. Without explicitly computing $\hat{K}$ (the dimensionality of which is in the square of tens of thousands, on the order of the number of surface points), λ_k and ϕ_k can be computed by singular value decomposition of the quantity $\sqrt{\Lambda}U$, where Λ is a diagonal matrix of the surface measures (Joshi et al., 1997). The Gaussian vector fields are then expanded as $u_i = \sum_k \alpha_{ik}\phi_k$, and the coefficients $Z = \{\alpha_i\}$, $\alpha_{ik} = <u_i, \phi_k> = \int_{\bar{\mathbf{M}}} u_i^T(x)\phi_k(x)dv(x)$ become independent Gaussian random variables with fixed means and covariances.

If the subject population is grouped into N_1 cases and N_2 controls, then the coefficient fields Z^1 and Z^2 (normally distributed with means $\bar{Z}^1$ and $\bar{Z}^2$, respectively) can be used to compare subcortical structure shapes across groups. The two groups of

subcortical structures are said to be different in shape if the null-hypothesis $H_0{:}\bar{Z}^1 = \bar{Z}^2$ on the empirical means

$$\hat{\bar{Z}}^1 = \frac{1}{N_1}\sum_{i=1}^{N_1} Z_i^1,$$

$$\hat{\bar{Z}}^2 = \frac{1}{N_2}\sum_{i=1}^{N_2} Z_i^2$$

with empirical common covariance

$$\hat{\Sigma} = \frac{1}{N_1+N_2-2}\left(\sum_{i=1}^{N_1}(Z_i^1-\hat{\bar{Z}}_i^1)(Z_i^1-\hat{\bar{Z}}_i^1)^T + \sum_{i=1}^{N_2}(Z_i^2-\hat{\bar{Z}}_i^2)(Z_i^2-\hat{\bar{Z}}_i^2)^T\right)$$

is rejected with a predetermined significance level (e.g., 0.05). To proceed, define Hötelling's T^2 statistic AS

$$T^2 = \frac{N_1N_2}{(N_1+N_2)}\left(\hat{\bar{U}}^1-\hat{\bar{U}}^2\right)^T\hat{\Sigma}^{-1}\left(\hat{\bar{U}}^1-\hat{\bar{U}}^2\right).$$

We note that the quantity $\sqrt{\frac{N_1N_2}{N_1+N_2}}(\hat{\bar{U}}^1-\hat{\bar{U}}^2)$ is normally distributed, and that the quantity $(N_1+N_2-2)\hat{\Sigma}$ is distributed as $\sum_{i=1}^{N_1+N_2-2}X_iX_i^T$ where X_i is normally distributed with zero mean and covariance Σ (Anderson, 1958, p. 109). Therefore, T^2 has an F distribution, and the null hypothesis H_0 is rejected with a significance level α if $T^2 \geq \frac{(N_1+N_2-2)K}{N_1+N_2-K-1}F^*_{K,N_1+N_2-K-1}(\alpha)$, where $F^*_{K,N_1+N_2-K-1}(\alpha)$ denotes the upper 100 α% point of the F_{K,N_1+N_2-K-1} distribution, and K is the total number of eigenfunctions used in calculating the T^2 statistics. The number of K eigenfunctions, in decreasing order of power, accounts for majority of the total variance (e.g., 75%). Logistic regression models based on χ^2 scoring of Z^1 and Z^2 can then be used to further determine a subset of eigenfunctions that maximally discriminate subject groups.

For nonparametric comparisons, Fisher's method of randomized permutation can be used. For all permutations of the given subject groups, the means and covariances are calculated from Monte Carlo simulations generating a large number (e.g., 10,000) of uniformly distributed random permutations. The collection of T^2 statistics from each permutation gives rise to an empirical distribution $\hat{F}$ using $F_{K,N_1+N_2-K-1} = \frac{N_1+N_2-K-1}{(N_1+N_2-2)K}T^2$ to estimate F. The null hypothesis H_0 is rejected when $p = \int_{T^2}^{\infty}\hat{F}\,(f)df$ falls below a predetermined significance level (e.g., 0.05). For an example, see Wang et al. (2001).

Methods for characterizing group differences of subregions of the cortical mantle

Our approach to the analysis of group differences in subregions of the cortical mantle (i.e., LCMDM) begins with a Bayesian segmentation of a subvolume of the MR image containing the selected cortical subregion using the expectation-maximization algorithm (Joshi et al., 1999). This algorithm fits compartmental statistics that segment the voxels of the subvolume into GM, WM, cerebrospinal fluid (CSF), partial CSF–gray (PCG), and partial gray–white (PGW) voxels. To resolve PCG and PGW voxels, expert manual segmentations of a subset of MR images are generated, and Neyman–Pearson likelihood ratio tests based on these manual segmentations are used to derive the optimal threshold with which to reclassify PCG and PGW voxels into GM, WM, or CSF voxels. We then generate smooth surfaces at the GM/WM interface by using isosurface generation algorithms (Miller et al., 2000, Ratnanather et al., 2001). Dynamic programming (Khaneja et al., 1998) is used to delineate the boundaries of the selected subregion of the cortical mantle (e.g., anterior cingulate gyrus, posterior cingulate gyrus) on the GM/WM interface surface. Cortical subregion surface areas are calculated by the sum of areas of each triangle in the triangulated isosurface subregion.

Probabilistic measures of the volume, thickness, and gray matter distribution of the selected subregion of the cortical mantle can also be characterized using LCMDM (Miller et al., 2003). Using an OcTree-based distance computing algorithm (Ratnanather et al., 2001), each nonbackground voxel is labeled by its distance to the nearest surface vertex and assigned to the delineated subregion of the cortical mantle. LCMDM defines the frequency occurrence of the labeled GM, WM, and CSF voxels as functions of distance to the GM/WM interface isosurface. To proceed, the 2D smooth interface surface $S(\Delta) \subset R^3$ is associated with a set of surface normal vectors at every point. Along the positive and negative surface normal directions (indicating either side of the surface) are points that are minimum distances defined by the set distance functions representing the distances between the center of the image voxels x and the surface $S(\Delta)$ (Ratnanather et al., 2001): $d(x) = \min_{s\in S(\Delta)}\|x-s\|$. The real-valued distances produce co-occurrence histograms for GM, WM, and CSF for each subregion in each subject. Cortical GM volumes are then calculated by summing the total histogram. Normalizing the histogram gives rise to a probability density function (PDF), and integrating the PDF gives rise a cumulative distribution function (CDF). Per subject average GM thickness can be defined as a percentile of the CDF (e.g., distance in mm at the 90th percentile).

Group differences in cortical gray matter distributions can be quantified using Wilcoxon–Mann–Whitney rank-sum tests on the CDFs for stochastic ordering, with the null hypothesis being that the distance values for the GM CDF for different groups come from the same distribution. Let X be a random variable represented by GM LCMDM with distribution F and Y a random variable with distribution H. X is said to be stochastically smaller than Y if $F(d) \leq H(d)$ for all d, with strict inequality for at least one d. Statistical significance from the rank-sum test indicates stochastic ordering of the two distributions and supports the hypothesis that the greater percentage of X GM voxels occupies smaller distances to the surface (i.e., cortical thinning).

Finally, the analysis of the topography of cortical thinning between groups of subjects requires quantifying between-subject cortical surface variation via surface matching (Thompson et al., 2000; Van Essen, 2002; Van Essen et al., 2001). In our case, smooth cortical GM/WM interface surfaces in the 3D image space are first mapped to 2D planar manifolds via discrete conformal mapping using circle packing (Hurdal et al., 1999). The anatomical landmarks used in the delineation of the selected subregions (see above) are carried onto the 2D planar manifolds. These surfaces can be matched by identifiable landmarks that correspond across subjects. Surface matching then deforms one surface so as to bring these landmarks into register. Let S be a cortical subregion surface with curvature κ_k of one subject and S' another with curvature κ'_k, the optimal matching $\hat{h} = \hat{\phi}^{-1}$

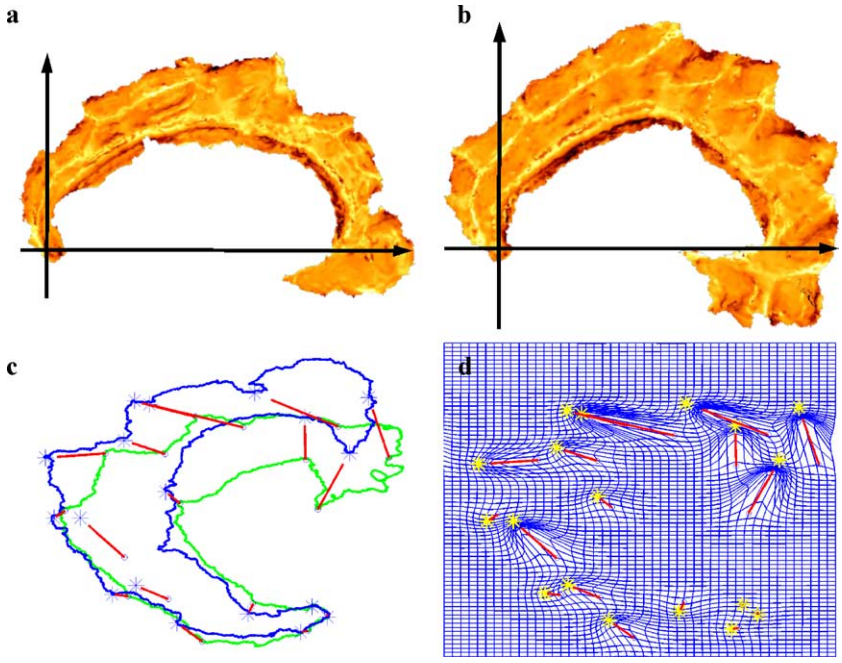

Fig. 1. Manifold mapping from 3D image space to 2D plane and manifold matching of the cingulate gyrus. Top row shows the cingulate gyrus GM/WM interface surface in 3D space mapped to a 2D plane in two subjects (panels a and b) via discrete conformal mapping using circle packing. Bottom row shows landmark-based manifold matching (panel c, red line indicates deformation of landmark from template surface-green to target surface-blue) and the resulting deformation field (panel d, Cartesian coordinate grid in the template under deformation).

is satisfied by: $\frac{d\hat{\phi}(t)}{dt} = \hat{v}\left(\hat{\phi}(t), t\right)$, where $\hat{\phi}(0) = \hat{\phi}^{-1}(0) = x$, $\hat{v}(\cdot) = \text{arginf}_v \|Lv\|^2 + \int_S \sum_{k=1}^{2} \left(\kappa_k\left(\phi^{-1}(1)\right) - \kappa'_k(x)\right) dm(x), m$ is the manifold measure, L is a linear differential operator, and $\|\cdot\|^2$ is the norm squared on functions indexed over S. This is a map restricted to the manifold taking corresponding landmark points from S to S'. We are currently developing this approach according to the principles described in Beg et al. (2003a) and Grenander and Miller (1998).

Fig. 1 shows an example of discrete conformal mapping and manifold matching of the cingulate gyrus surface. The 3D cingulate gyrus is mapped into a 2D plane to facilitate between-subject manifold mapping.

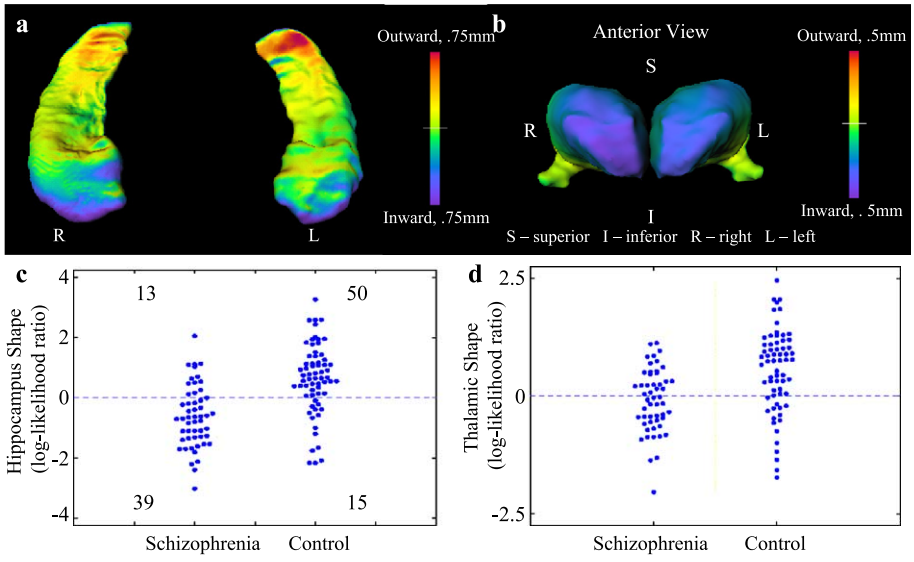

Fig. 2. Structural differences of the hippocampus and the thalamus in schizophrenia. Top row shows differences in hippocampal surface patterns between schizophrenia and control groups (panel a) and differences in thalamic surface patterns between the same groups (panel b), visualized as differences with direction (inward vs. outward) on the mean surfaces. Inward surface deformations are visualized in cooler colors and outward surface deformations in warmer colors. Bottom row shows the group differences as log-likelihood ratio statistics based on shape decomposition for the hippocampus (panel c, using hippocampal eigenfunctions 1, 5, and 14), and for the thalamus (panel d, using thalamic eigenfunctions 1, 8, and 10).

Detecting differences in subcortical structures in schizophrenia subjects and healthy controls

Our studies of subjects with schizophrenia exemplify our methods for characterizing group differences in neuroanatomical shapes. As mentioned above, we detected and quantified abnormalities of the shape of the hippocampus and thalamus in 52 subjects with schizophrenia as compared to 65 healthy subjects matched for age, gender, and parental socioeconomic status (Csernansky et al., 2002; Csernansky et al., 2004b). In both of these brain structures, we found distinct patterns of inward deformities that could account for the small decreases in structural volumes reported by others (see above). For example, the pattern of hippocampal shape difference between the schizophrenia subjects as compared to healthy controls indicates a highly localized loss of volume in the head of the hippocampus (see Fig. 2). Also, the pattern of thalamic shape difference between the same two groups of subjects suggests a loss of volume in the extreme anterior and posterior regions of the thalamus. We are currently engaged in further research to determine the cellular basis and functional consequences of these shape changes, and whether such shape changes are specific to schizophrenia.

Moreover, we found that combining shape information from the hippocampus and the thalamus together improved our ability to discriminate between these groups of subjects. Examining the shape of the hippocampus alone, the combination of hippocampal eigenfunctions 1, 5, and 14 correctly classified 59.6% of the schizophrenia subjects and 80.0% of the control subjects. In turn, examining the shape of the thalamus alone, the combination of thalamic eigenfunctions 1, 8, and 10 correctly classified 53.4% of the schizophrenia subjects and 75.4% of the control subjects. Thus, examining the shape of these two structures separately allowed us to correctly classify the large majority of healthy control subjects, but not the substantial majority of subjects with schizophrenia. Fortunately, however, the combination of hippocampal eigenfunctions 1, 5, 14 and thalamic eigenfunctions 8 and 10 improved the classification accuracy to 73.1% for the schizophrenia subjects and 83.1% for the control subjects. Also, the correlations of eigen coefficients between the left and right hippocampus or the left and right thalamus in both groups of subjects were very high (r = 0.86–0.92), while correlations of eigen coefficients between the hippocampus and thalamus or the left or right were lower in both groups of subjects (r = 0.52–0.64).

These results are consistent with previous reports of decreased neuroanatomical volumes in patients with schizophrenia (see above), but extend these studies by defining the abnormalities of neuroanatomical shape that are associated with volume losses. Our finding that combining shape information from multiple structures improves clinical classification (and especially of the schizophrenia subjects) suggests that schizophrenia is heterogeneous at least with respect to the presence or distribution of neuroanatomical abnormalities. Although individuals with schizophrenia may share common clinical features, the underlying cognitive deficits associated with such clinical features may be derived from abnormal functional networks of connected neuroanatomical structures (Barch et al., 2002). Thus, the neuroanatomical abnormalities associated with common clinical and cognitive deficits may differ in different subgroups of individuals with schizophrenia.

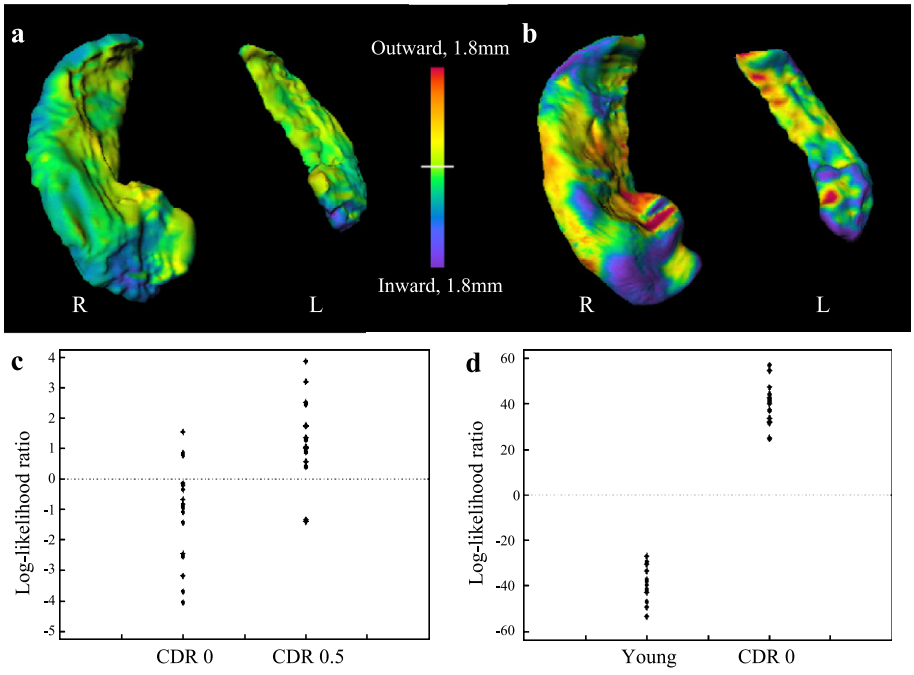

Fig. 3. Healthy aging vs. very mild DAT. Top row shows differences in hippocampal surface patterns between mild DAT and elderly control groups (panel a, DAT), and between the elderly and younger controls groups (panel b, healthy aging), visualized as differences with direction (inward vs. outward) on the mean surfaces. Inward surface deformations are visualized in cooler colors and outward surface deformation in warmer colors. Bottom row shows the group differences as log-likelihood ratio statistics based on shape decomposition for the mild DAT and elderly control groups (panel c, using eigenfunction 5 together with left and right hippocampal volumes), and for the elderly and younger controls groups (panel d, using eigenfunctions 1 and 2 together with left and right hippocampal volumes).

Discriminating AD from healthy aging

In a study of 18 subjects with very mild DAT, 18 healthy elderly, and 15 healthy younger subjects, we found that hippocampal volume and shape information could be used in a complementary fashion to discriminate between groups (Csernansky et al., 2000). When comparing DAT and elderly control groups, eigenfunction 5 combined with left and right hippocampal volumes achieved the highest classification accuracy (83% of DAT subjects and 78% of healthy elderly subjects) as compared to the classification of subjects based on volume alone or eigen coefficients alone. To determine whether there were changes in hippocampal structure associated with healthy aging, we then compared the healthy elderly and younger subjects. In this case, there was no significant difference in hippocampal volumes, and a different set of shape eigenfunctions (1 and 2) discriminated the groups (with or without inclusion of volume).

The pattern of hippocampal surface difference in subjects with very mild DAT vs. healthy elderly subjects was consistent with neurodegeneration of the CA1 hippocampal subfield (see Fig. 3), which has been observed in postmortem studies of subjects with early forms of AD (Arnold et al., 1991; Price and Morris, 1999). However, the pattern of hippocampal surface difference that discriminated the healthy elderly and healthy younger subjects was associated with a shape change quite distinct from that associated with AD and without any substantial volume loss. These results suggest that AD and healthy aging are associated with distinct effects on hippocampal structure, perhaps based on distinct neurobiological processes.

Detecting group difference in subregions of the cortical mantle in AD

We have recently used LCMDM to assess the gray matter volume, thickness, and surface area of the cingulate gyrus in 9 subjects with mild DAT, 8 subjects with very mild DAT, 10 healthy elderly, and 10 younger control subjects (Miller et al., 2003). We observed significantly smaller gray matter volumes in the mild and very mild DAT groups in both the anterior and posterior segments of the cingulate gyrus. We also observed a significant difference between the groups of DAT subjects and the groups of healthy subjects in the gray matter distribution functions in the posterior cingulate gyrus, which suggested that early AD is also associated with regional thinning of the cortical mantle. In contrast, we found no significant difference between the healthy elderly and younger subjects in either gray matter volume or the cortical mantle shape.

Fig. 4 summarizes the results from this study. Cortical mantle distribution curves yielded measures of both volume and thickness. Apparent "shifts" in the distribution curves, which indicate cortical mantle thinning, were confirmed by the testing of stochastic ordering. These results suggest that the gray matter volume loss and thinning of the posterior cingulate gyrus may be a feature of early AD, but not of healthy aging. Again, postmortem studies suggest that the neuropathological features of AD (i.e., plaques and tangles) are prominent in this region of the cerebral cortex (Arnold et al., 1991).

Statistical inferences on neuroanatomical asymmetry

As mentioned above, another approach to detecting and characterizing neuroanatomical abnormalities in patients with neuropsychiatric disorders is to look for group differences in the relationships between neuroanatomical structures. As a special case of this problem, one can quantify and compare the hemispheric asymmetries of paired neuroanatomical structures in subjects with neuropsychiatric disorders vs. healthy controls.

Quantification of the asymmetry of paired neuroanatomical structures in groups of subjects is based on side-to-side mappings (Wang et al., 2001). Let h^l and h^r be transformations of the template into the left and right hemisphere, respectively, for each subject. Then, reflecting from right to left (left to right is the

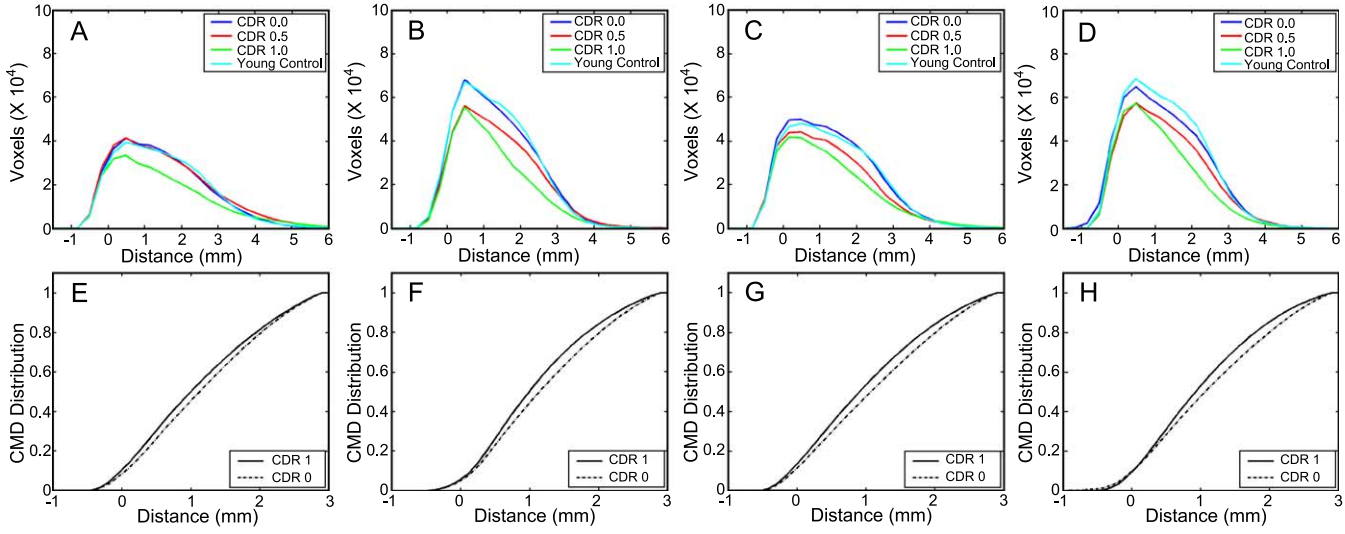

Fig. 4. Labeled cortical mantle distance maps of the cingulate gyrus in DAT. Top row shows averages of gray matter histograms as a function of distance from the GM/WM interface surfaces for left anterior (panel A), right anterior (panel B), left posterior (panel C), and right posterior (panel D) segments of the cingulate gyrus. The groups are subjects with mild DAT (rated as 1 on the Clinical Dementia Rating scale [CDR]), very mild DAT (rated as 0.5 on the CDR), healthy elderly (rated as 0 on the CDR), and younger control (YC) subjects. Bottom row shows the average cortical mantle CDF differences comparing the mild DAT and healthy aging groups (panels E–H) in the corresponding regions. The apparent "shifts" in the distribution curves were confirmed by significant levels in the stochastic ordering and therefore indicate a significant change in cortical mantle shape (i.e., thinning).

mathematical inverse), within-subject structural asymmetry is defined as $u = f(h^r) - h^l$, where f is the rigid motion inversion. While $u = 0$ implies perfect symmetry, we can quantify normative asymmetry by variations away from zero and abnormal asymmetry as the degree to which this normative asymmetry is altered in subjects with a particular neuropsychiatric disorder.

Based on the eigen decomposition approaches for subcortical structures (see Section 0), the decomposition of uu^T gives rise to vector coefficients Z with covariance Σ. We therefore define asymmetry metric for each subject as $a_i B\sqrt{Z_i^T \Sigma^{-1} Z_i}$ and define the group asymmetry metric as $\bar{a} B\sqrt{Z^T \Sigma^{-1} Z}$. Clearly,1 $\bar{a} = 0$ indicates perfect symmetry, with larger values of a indicating more asymmetry.

Abnormal asymmetry of subcortical structures in schizophrenia

Because schizophrenia has been hypothesized to be a neurodevelopmental disorder and because neurodevelopment establishes the normative asymmetry of paired structures, exaggerations or reversals of normative asymmetries may also help to define the neuroanatomical basis of schizophrenia. In our study of 52 subjects with schizophrenia and 65 control subjects (see Section 0), we found that the hippocampus in both the schizophrenia and control subjects showed a significant hemispheric asymmetry in shape (schizophrenia asymmetry metric = 2.24 with asymmetry eigenfunctions 5 and 13, control asymmetry metric = 2.17 with asymmetry eigenfunctions 5 and 13). Thalamic asymmetry in both groups was smaller, but still measurable (schizophrenia asymmetry metric = 0.66 with asymmetry eigenfunctions 6 and 16, control asymmetry metric = 0.52 with asymmetry eigenfunctions 12 and 13).

Fig. 5 illustrates several results from this study. The left hippocampus had a less prominent lateral surface and exaggerated bending along its longitudinal axis compared with the right in both schizophrenia and control subjects. In turn, the left thalamus was slightly smaller than the right in the dorsal–medial portion of its surface. However, comparing schizophrenia and control subjects, there was an exaggeration of these normative (L < R) patterns of hippocampal and thalamic asymmetry in the subjects with schizophrenia. This finding is consistent with prior reports that volume losses are more prominent on the left side of the brain in subjects with schizophrenia (McCarley et al., 1993; Shenton et al., 1992).

Statistical inferences on time-dependent changes

The assessment of changes in neuroanatomical structure over time is especially useful for characterizing the trajectory of neuropsychiatric disorders that are progressive (e.g., degenerative) in nature. Quantification of time-dependent neuroanatomical change is based on within-subject mappings (Wang et al., 2003).

Let h^{t_1} and h^{t_2} be transformations of the template at two time points, respectively, for each subject. Removing rotation and translation effects of intrasubject scanner-related changes, the structural change between time points is then defined as $u = h^{t_2} - h^{t_1}$. While $u = 0$ implies a perfectly unchanged brain structure, the normative pattern of change can be quantified by variations away from zero and neurodegeneration as the degree to which this normative pattern of change is altered in subjects with a particular neuropsychiatric disorder.

Based on the eigen decomposition approaches for subcortical structures, the decomposition of uu^T gives rise to vector coefficients Z with covariance Σ. We therefore define a change metric for each subject as: $c_i B\sqrt{Z_i^T \Sigma^{-1} Z_i}$, and define the group change metric as $\bar{c} B\sqrt{Z^T \Sigma^{-1} Z}$. Clearly, $\bar{c} = 0$ indicates no shape change over time, with larger values of c indicating more shape change.

Progressive shape change (degeneration) of the hippocampus in AD

As an example of making a statistical inference on time-dependent change in the shape of the hippocampus, we used HDBM-LD to conduct a 2-year longitudinal study of 18 subjects

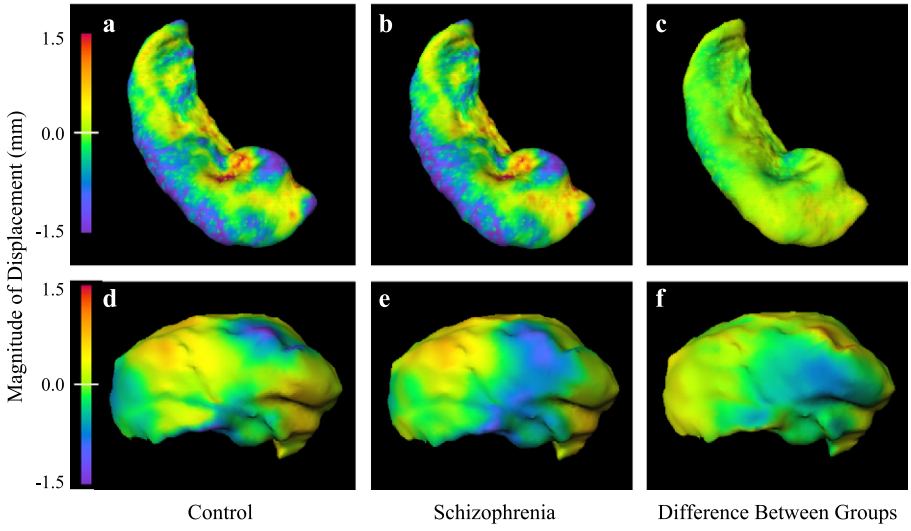

Fig. 5. Exaggerated asymmetries of the hippocampus and thalamus in schizophrenia. Top row shows patterns of hippocampal asymmetry for schizophrenia and control groups (panels a and b) and between-group comparisons of hippocampal asymmetry (panel c). Bottom row shows patterns of thalamic asymmetry for the same schizophrenia and control groups (panels d and e) and between-group comparisons of thalamic asymmetry (panel f). Inward surface deformations are visualized in cooler colors, outward in warmer colors, and undeformed areas in neutral yellow-to-green.

with very mild DAT and 26 healthy elderly subjects (Wang et al., 2003). In healthy elderly subjects, we observed nonsignificant decreases in hippocampal volume (left: 4.0%; right: 5.5%) and a mild shape change (change metric = 1.0 with change eigenfunctions 8 and 11). However, subjects with very mild DAT showed larger and significant decreases in hippocampal volume (left: 8.3%, $P = 0.03$; right: 10.2%, $P = 0.05$) and a more substantial shape change (change metric = 1.7 with change eigenfunctions 1, 4, and 8). Rates of change in both hippocampal volume and shape could be used to distinguish the DAT and healthy elderly subjects, and when information about volume and shape change were combined, we were able to classify 72.2% of the subjects with DAT and 96.2% of the healthy elderly subjects. At baseline, the subjects with very mild DAT showed an inward deformation over 38% of the hippocampal surface compared with the healthy elderly group. However, after 2 years, 47% of the hippocampal surface showed an inward deformation in the DAT subjects compared to the healthy elderly subjects.

Fig. 6 summarizes the patterns of time-dependent hippocampal shape change associated with AD. The DAT and healthy aging subjects were characterized by different patterns of hippocampal shape change. In the healthy elderly subjects, small areas of inward deformation were observed in the region of the head of the hippocampus, on scattered areas of the lateral surface of the body of the hippocampus, and in the region of the subiculum. In the subjects with very mild DAT, the progressive change in shape engulfed most of the head of the hippocampus and the lateral aspect of the body. As noted above, this portion of the hippocampal surface overlies the CA1 subfield and the subiculum, which are regions that show early evidence of AD neuropathology in postmortem studies (Arnold et al., 1991; Price and Morris, 1999). Also, our findings are consistent with and extend several prior studies where rates of change in the gray matter volume of the hippocampus and related structures were found to differ between subjects with DAT and controls (Fox et al., 1996a; Jack et al., 1998).

Discussion

CA offers new approaches to detecting and quantifying abnormalities of brain structure in groups of subjects with neuropsychiatric disorders. Because metrics other than volumes can be generated, abnormalities of neuroanatomical structures that are associated with neuropsychiatric disorders, but not necessarily with changes in the overall size of such structures, can be detected and quantified. With regard to subcortical structures, an analysis of the surfaces that enclose them allows for the characterization of abnormalities of shape and asymmetry at one point in time or over several points in time. With regard to the subregions of the cortical mantle, an analysis of the cortical mantle in anatomical relationship to a surface representing the interface between GM and WM allows for the independent measurement of GM volume, surface area, thickness, and the contouring of the cortical mantle within a specific subregion.

The assessment of group differences in individual structures, patterns of asymmetry, and time-dependent changes in structures has allowed us to discriminate subjects with schizophrenia and very mild forms of AD from relevant control groups. In particular, combining information from multiple structures and assessing cortical volumes and thickness together within a predefined subregion of the cortical mantle appear to optimize the classification of subjects with these neuropsychiatric disorders. As CA is

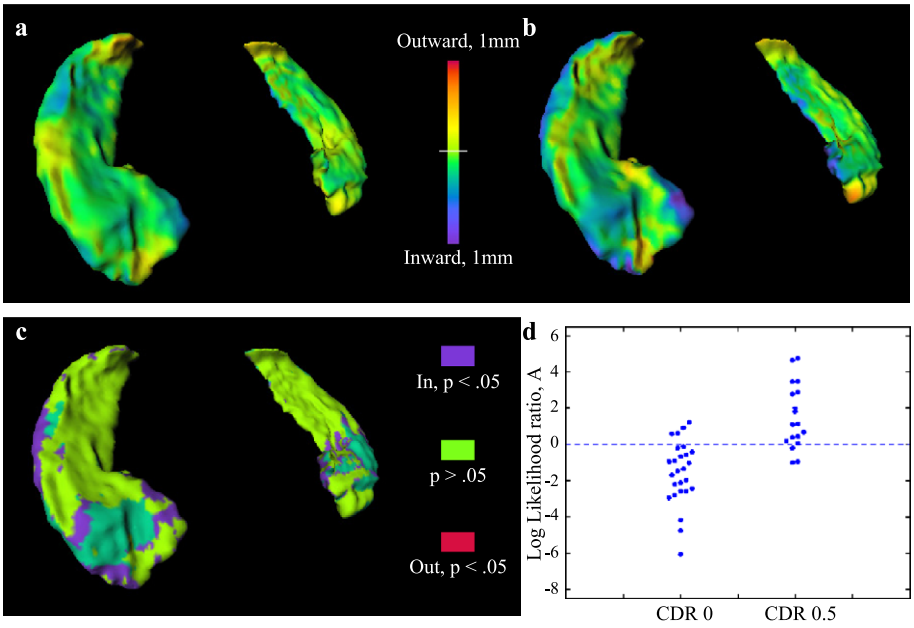

Fig. 6. AD vs. healthy-structural changes of the hippocampus over time. Top row shows patterns of hippocampal change over a 2-year period in healthy elderly subjects (panel a) and in subjects with very mild DAT (panel b). Inward surface deformations are visualized in cooler colors, outward in warmer colors, and undeformed areas in neutral yellow-to-green. Bottom row shows the "spread" of the between-group inward surface deformation patterns over 2 years (panel c), shown as a Wilcoxon's sign rank test map on the mean surface of healthy elderly subjects (i.e., rated as 0 on the CDR). Areas of significant ($P < 0.05$) inward deformation at baseline in subjects rated as 0.5 on the CDR subjects are shown in turquoise and represent 38% of total hippocampal surface area. After 2 years, the areas of significant inward deformation have grown to represent 47% of the total hippocampal surface. Areas where inward deformation developed over time are shown in purple, and areas of nonsignificant change in shape are shown in green. Bottom row shows the sufficient statistics for the linear combination of eigenfunctions 1, 2, 4, and 11, which discriminated rates of shape change between the two subject groups (panel d).

continuously applied to the analysis of more brain structures, we will eventually develop a more complete understanding of the neuroanatomical disturbances that are characteristic of these and other neuropsychiatric disorders.

A thorough understanding of the pattern of neuroanatomical abnormalities in a given neuropsychiatric disorder can help guide investigations of the physiology of specific neuronal circuits that play critical roles in producing functional deficits. Because of the precision of CA methods and the richness of the measures that can be derived from them, these methods should also be ideal for detecting and characterizing neuroanatomical abnormalities in individuals with preclinical forms of neuropsychiatric disorders. Also, specific patterns of neuroanatomical variation might be associated with the capacity to respond to particular treatment interventions.

Acknowledgments

The authors acknowledge support from PHS grants MH56584 and MH60883, the Silvio Conte Center at Washington University School of Medicine (MH 62130), NIH PO1-CA47982, and the F. M. Kirby Research Center for Functional Brain Imaging (1 P41 RR15241-01A1).

References

Altshuler, L.L., Casanova, M.F., Goldberg, T.E., Kleinman, J.E., 1990. The hippocampus and parahippocampus in schizophrenic, suicide, and control brains. Arch. Gen. Psychiatry 47, 1029–1034.

Anderson, T.W., 1958. An Introduction to Multivariate Statistical Analysis. Wiley, New York.

Andreasen, N.C., 1984. The Scale for Assessment of Positive Symptoms (SAPS). The University of Iowa, Iowa City, IA.

Andreasen, N.C., Nasrallah, H.A., Dunn, V., et al., 1986. Structural abnormalities in the frontal system in schizophrenia: a magnetic resonance imaging study. Arch. Gen. Psychiatry 43, 136–144.

Arnold, S.E., Hyman, B.T., Flory, J., Damasio, A.R., Van Hoesen, G.W., 1991. The topographical and neuroanatomical distribution of neurofibrillary tangles and neuritic plaques in the cerebral cortex of patients with Alzheimer's disease. Cereb. Cortex 1, 103–116.

Ashburner, J., Csernansky, J.G., Davatzikos, C., Fox, N.C., Frisoni, G.B., Thompson, P.M., 2003. Computer-assisted imaging to assess brain structure in healthy and diseased brains. Lancet Neurol. 2, 79–88.

Barch, D.M., Csernansky, J.G., Conturo, T., Snyder, A.Z., 2002. Working and long-term memory deficits in schizophrenia: is there a common prefrontal mechanism? J. Abnorm. Psychology 111, 478–494.

Beg, M.F., Miller, M.I., Trouve, A., Younes, L., 2003a. The Euler–Lagrange equation for interpolating sequence of landmark datasets. In: Ellis, R.E., Peters, T.M. (Eds.), MICCAI 2003, LNCS 2879. Springer-Verlag, Berlin Heidelberg, pp. 918–925.

Beg, M.F., Miller, M.I., Younes, L., Trouvé, A., 2003b. Computing metrics on flows of diffeomorphisms. Int. J. Comput. Vis. (in press).

Benes, F.M., Sorensen, I., Bird, E.D., 1991. Reduced neuronal size in posterior hippocampus of schizophrenic patients. Schizophr. Bull. 17, 597–608.

Bookstein, F.L., 1978. The measurement of biological shape and shape change. Lect. Notes Biomath. vol 24. Springer-Verlag, New York.

Bookstein, F.L., Green, W.D.K., 1992. Edge information at landmarks in medical images. In: Robb, R.A. (Ed.), Visualization in Biomedical Computing., Proceedings of SPIE, Chapel Hill, NC, pp. 242–258.

Boothby, W.M., 1986. An Introduction to Differentiable Manifolds and Riemannian Geometry. Academic Press, Orlando, FL.

Buchsbaum, M.S., Someya, T., Teng, C.Y., et al., 1996. PET and MRI of the thalamus in never-medicated patients with schizophrenia. Am. J. Psychiatry 153, 191–199.

Byne, W., Buchsbaum, M.S., Mattiace, L.A., et al., 2002. Postmortem assessment of thalamic nuclear volumes in subjects with schizophrenia. Am. J. Psychiatry 159, 59–65.

Cannon, T.D., van Erp, T.G., Bearden, C.E., et al., 2003. Early and late neurodevelopmental influences in the prodrome to schizophrenia: contributions of genes, environment, and their interactions. Schizophr. Bull. 29, 653–669.

Christensen, G.E., Rabbitt, R.D., Miller, M.I., 1993. A deformable neuroanatomy textbook based on viscous fluid mechanics. In: Prince, J., Runolfsson, T. (Eds.), 27th Annual Conference on Information Sciences and Systems. Johns Hopkins University, Baltimore, Maryland, pp. 211–216.

Christensen, G.E., Rabbitt, R.D., Miller, M.I., 1994. 3D brain mapping using a deformable neuroanatomy. Phys. Med. Biol. 39, 609–618.

Christensen, G.E., Rabbitt, R.D., Miller, M.I., Joshi, S.C., Grenander, U., Coogan, T.A., 1995. Topological Properties of Smooth Anatomical Maps. Kluwer Academic Publishers, Boston, pp. 101–112.

Csernansky, J.G., Joshi, S., Wang, L., et al., 1998. Hippocampal morphometry in schizophrenia by high dimensional brain mapping. Proc. Natl. Acad. Sci. U. S. A. 95, 11406–11411.

Csernansky, J.G., Wang, L., Joshi, S., et al., 2000. Early DAT is distinguished from aging by high-dimensional mapping of the hippocampus. Neurology 55, 1636–1643.

Csernansky, J.G., Wang, L., Jones, D., et al., 2002. Hippocampal deformities in schizophrenia characterized by high dimensional brain mapping. Am. J. Psychiatry 159, 2000–2006.

Csernansky, J.G., Hamstra, J., Wang, L., et al., 2004a. Correlations between antemortem hippocampal volume and postmortem neuropathology in AD subjects. Alzheimer Dis. Assoc. Disord. (in press).

Csernansky, J.G., Schlinder, M.K., Splinter, N.R., et al., 2004b. Abnormalities of thalamic volume and shape in schizophrenia. Am. J. Psychiatry 161, 896–902.

Dale, A.M., Fischl, B., Sereno, M.I., 1999. Cortical surface-based analysis: I. Segmentation and surface reconstruction. NeuroImage 9, 179–194.

Du, A.T., Schuff, N., Zhu, X.P., et al., 2003. Atrophy rates of entorhinal cortex in AD and normal aging. Neurology 60, 481–486.

Evans, A.C., Dai, W., Collins, L., Neelin, P., Marrett, S., 1991. Warping of a computerized 3D atlas to match brain image volumes for quantitative neuroanatomical and functional analysis. Image Process. 1445, 236–246.

Falkai, P., Bogerts, B., 1986. Cell loss in the hippocampus of schizophrenics. Eur. Arch. Psychiatr. Neurol. Sci. 236, 154–161.

Fischl, B., Salat, D.H., Busa, E., et al., 2002. Whole brain segmentation: automated labeling of neuroanatomical structures in the human brain. Neuron 33, 341–355.

Fox, N.C., Freeborough, P.A., 1997. Brain atrophy progression measured from registered serial MRI: validation and application to Alzheimer's disease. J. Magn. Reson. Imaging 7, 1069–1075.

Fox, N.C., Freeborough, P.A., Rossor, M.N., 1996a. Visualisation and quantification of rates of atrophy in Alzheimer's disease [see comments]. Lancet 348, 94–97.

Fox, N.C., Warrington, E.K., Freeborough, P.A., et al., 1996b. Presymptomatic hippocampal atrophy in Alzheimer's disease. A longitudinal MRI study. Brain 119, 2001–2007.

Fox, N.C., Cousens, S., Scahill, R., Harvey, R.J., Rossor, M.N., 2000. Using serial registered brain magnetic resonance imaging to measure disease progression in Alzheimer disease: power calculations and estimates of sample size to detect treatment effects. Arch. Neurol. 57, 339–344.

Fox, N.C., Crum, W.R., Scahill, R.I., Stevens, J.M., Janssen, J.C., Rossor, M.N., 2001. Imaging of onset and progression of Alzheimer's disease with voxel-compression mapping of serial magnetic resonance images. Lancet 358, 201–205.

Freeborough, P.A., Fox, N.C., 1998. Modeling brain deformations in

Alzheimer disease by fluid registration of serial 3D MR images. J. Comput. Assist. Tomogr. 22, 838–843.
Giguere, M., Goldman-Rakic, P.S., 1988. Mediodorsal nucleus: areal, laminar, and tangential distribution of afferents and efferents in the frontal lobe of rhesus monkeys. J. Comp. Neurol. 277, 195–213.
Good, C.D., Johnsrude, I.S., Ashburner, J., Henson, R.N., Friston, K.J., Frackowiak, R.S., 2001. A voxel-based morphometric study of ageing in 465 normal adult human brains. NeuroImage 14, 21–36.
Greitz, T., Bohm, C., Holte, S., Eriksson, L., 1991. A computerized brain atlas: construction, anatomical content, and some applications. J. Comput. Assist. Tomogr. 15, 26–38.
Grenander, U., Miller, M.I., 1994. Representations of knowledge in complex systems. J. R. Stat. Soc., B 56, 549–603.
Grenander, U., Miller, M.I., 1998. Computational anatomy: an emerging discipline. Q. Appl. Math. LVI, 617–694.
Gur, R.E., Cowell, P.E., Turetsky, B.I., et al., 1998. A follow-up magnetic resonance imaging study of schizophrenia. Arch. Gen. Psychiatry 55, 145–152.
Hurdal, M.K., Bowers, P.L., Stephenson, K., et al., 1999. Quasi-conformally flat mapping the human cerebellum. Medical Image Computing and Computer-Assisted Intervention-MICCAI99.
Hyman, B.T., Van Hoesen, G.W., Damasio, A.R., 1987. Alzheimer's disease: glutamate depletion in the hippocampal perforant pathway zone. Ann. Neurol. 22, 37–40.
Jack Jr., C.R., Petersen, R.C., Xu, Y., O'Brien, P.C., Smith, G.E., Ivnik, R.J., Tangalos, E.G., Kokmen, E., 1998. Rate of medial temporal lobe atrophy in typical aging and Alzheimer's disease. Neurology 51, 993–999.
Jansen, W., Baak, J.P., Smeulders, A.W., van Ginneken, A.M., 1989. A computer based handbook and atlas of pathology. Pathol. Res. Pract. 185, 652–656.
Jeste, D.V., Lohr, J.B., 1989. Hippocampal pathologic findings in schizophrenia. A morphometric study. Arch. Gen. Psychiatry 46, 1019–1024.
Joshi, S., Wang, J., Miller, M.I., Van Essen, D.C., Grenander, U., 1995a. On the differential geometry of the cortical surface. Int'l. Symp. on Optical Science, Engineering, and Instrumentation.
Joshi, S., Miller, M.I., Christensen, G.E., Coogan, T.A., Grenandur, U., 1995b. The generalized dirichlet problem for mapping brain manifolds. Int'l Symp on Optical Science, Engineering, and Instrumentation.
Joshi, S., Miller, M.I., Grenander, U., 1997. On the geometry and shape of brain sub-manifolds. Int. J. Pattern Recogn. Artif. Intell. 11, 1317–1343. (Special Issue).
Joshi, M., Cui, J., Doolittle, K., et al., 1999. Brain segmentation and the generation of cortical surfaces. NeuroImage 9, 461–476.
Khaneja, N., Grenander, U., Miller, M.I., 1998. Dynamic programming generation of curves on brain surfaces. IEEE Trans. Pattern Anal. Mach. Intell. 20, 1260–1264.
Manaye, K., German, D., Liang, C.-L., Hicks, P., Young, K., 1997. Reduced number of mediodorsal thalamic neurons in schizophrenics. Soc. Neurosci. Abst. 23, 2200.
McCarley, R.W., Shenton, M.E., O'Donnell, B.F., et al., 1993. Auditory P300 abnormalities and left posterior superior temporal gyrus volume reduction in schizophrenia. Arch. Gen. Psychiatry 50, 190–197.
Miller, M.I., Christensen, G.E., Amit, Y., Grenander, U., 1993. Mathematical textbook of deformable neuroanatomies. Proc. Natl. Acad. Sci. U. S. A. 90, 11944–11948.
Miller, M.I., Banerjee, A., Christensen, G.E., et al., 1997. Statistical methods in computational anatomy. Stat. Methods Med. Res. 6, 267–299.
Miller, M.I., Massie, A.B., Ratnanather, J.T., Botteron, K.N., Csernansky, J.G., 2000. Bayesian construction of geometrically based cortical thickness metrics. NeuroImage 12, 676–687.
Miller, M.I., Trouve, A., Younes, L., 2002. On the metrics and Euler–Lagrange equations of computational anatomy. Annu. Rev. Biomed. Eng. 4, 375–405.
Miller, M.I., Hosakere, M., Barker, A.R., et al., 2003. Labelled cortical mantle distance maps in the cingulate quantify cortical differences distinguishing dementia of the Alzheimer type and healthy aging. Proc. Nat. Acad. Sci. 100, 15172–15177.
Mungas, D., Reed, B.R., Jagust, W.J., DeCarli, C., Mack, W.J., Kramer, J.H., Weiner, M.W., Schuff, N., Chui, H.C., 2002. Volumetric MRI predicts rate of cognitive decline related to AD and cerebrovascular disease. Neurology 59, 867–873.
Nelson, M.D., Saykin, A.J., Flashman, L.A., Riordan, H.J., 1998. Hippocampal volume reduction in schizophrenia as assessed by magnetic resonance imaging: a meta-analytic study. Arch. Gen. Psychiatry 55, 433–440.
Pakkenberg, B., 1990. Pronounced reduction of total neuron number in mediodorsal thalamic nucleus and nucleus accumbens in schizophrenics. Arch. Gen. Psychiatry 47, 1023–1028.
Price, J.L., Morris, J.C., 1999. Tangles and plaques in nondemented aging and "preclinical" Alzheimer's disease. Ann. Neurol. 45, 358–368.
Rajkowska, G., Selemon, L.D., Goldman-Rakic, P.S., 1998. Neuronal and glial somal size in the prefrontal cortex: a postmortem morphometric study of schizophrenia and Huntington disease. Arch. Gen. Psychiatry 55, 215–224.
Ratnanather, J.T., Botteron, K.N., Nishino, T., et al., 2001. Validating cortical surface analysis of medial prefrontal cortex. NeuroImage 14, 1058–1069.
Romanski, L.M., Giguere, M., Bates, J.F., Goldman-Rakic, P.S., 1997. Topographic organization of medial pulvinar connections with the prefrontal cortex in the rhesus monkey. J. Comp. Neurol. 379, 313–332.
Scheltens, P., Fox, N., Barkhof, F., De Carli, C., 2002. Structural magnetic resonance imaging in the practical assessment of dementia: beyond exclusion. Lancet Neurol. 1, 13–21.
Selemon, L.D., Rajkowska, G., Goldman-Rakic, P.S., 1998. Elevated neuronal density in prefrontal area 46 in brains from schizophrenic patients: application of a three-dimensional, stereologic counting method. J. Comp. Neurol. 392, 402–412.
Selemon, L.D., Kleinman, J.E., Herman, M.M., Goldman-Rakic, P.S., 2002. Smaller frontal gray matter volume in postmortem schizophrenic brains. Am. J. Psychiatry 159, 1983–1991.
Shattuck, D.W., Sandor-Leahy, S.R., Schaper, K.A., Rottenberg, D.A., Leahy, R.M., 2001. Magnetic resonance image tissue classification using a partial volume model. NeuroImage 13, 856–876.
Shenton, M.E., Kikinis, R., Jolesz, F.A., et al., 1992. Abnormalities of the left temporal lobe and thought disorder in schizophrenia. A quantitative magnetic resonance imaging study. N. Engl. J. Med. 327, 604–612.
Sowell, E.R., Levitt, J., Thompson, P.M., et al., 2000. Brain abnormalities in early-onset schizophrenia spectrum disorder observed with statistical parametric mapping of structural magnetic resonance images. Am. J. Psychiatry 157, 1475–1484.
Sowell, E.R., Peterson, B.S., Thompson, P.M., Welcome, S.E., Henkenius, A.L., Toga, A.W., 2003. Mapping cortical change across the human life span. Nat. Neurosci. 6, 309–315.
Squire, L.R., Zola-Morgan, S., 1991. The medial temporal lobe memory system. Science 253, 1380–1386.
Suddath, R.L., Casanova, M.F., Goldberg, T.E., Daniel, D.G., Kelsoe, J.R., Weinberger, D.R., 1989. Temporal lobe pathology in schizophrenia: a quantitative MRI study. Am. J. Psychiatry 146, 464–472.
Thompson, P.M., Schwartz, C., Toga, A.W., 1996. High-resolution random mesh algorithms for creating a probabilistic 3D surface atlas of the human brain. NeuroImage 3, 19–34.
Thompson, P.M., MacDonald, D., Mega, M.S., Holmes, C.J., Evans, A.C., Toga, A.W., 1997. Detection and mapping of abnormal brain structure with a probabilistic atlas of cortical surfaces. J. Comput. Assist. Tomogr. 21, 567–581.
Thompson, P.M., Mega, M.S., Woods, R.P., et al., 2000. Early cortical change in Alzheimer's disease detected with a disease-specific, population-based, probabilistic brain atlas. Neurology 54, A475–A476.
Toga, A.W., Banerjee, P.K., Payne, B.A., 1991. Brain warping and averaging. J. Cereb. Blood Flow Metab. 11, S560.

Toga, A.W., Thompson, P.M., Payne, B.A., 1996. Modeling morphometric changes of the brain during development. In: Thatcher, R.W., Lyon, G.R., Rumsey, J., Krasnegor, N. (Eds.), Developmental Neuroimaging: Mapping the Development of the Brain and Behavior. Academic Press, New York, pp. 15–27.

Van Essen, D.C., 1997. A tension-based theory of morphogenesis and compact wiring in the central nervous system. Nature 385, 313–318.

Van Essen, D.C., 2002. Surface-based atlases of cerebellar cortex in the human, macaque, and mouse. Ann. N. Y. Acad. Sci. 978, 468–479.

Van Essen, D.C., Maunsell, J.H.R., 1980. Two-dimensional maps of the cerebral-cortex. J. Comp. Neurol. 191, 255–281.

Van Essen, D.C., Drury, H.A., Joshi, S., Miller, M.I., 1998. Functional and structural mapping of human cerebral cortex: solutions are in the surfaces. Proc. Natl. Acad. Sci. U. S. A. 95, 788–795.

Van Essen, D.C., Lewis, J.W., Drury, H.A., et al., 2001. Mapping visual cortex in monkeys and humans using surface-based atlases. Vis. Res. 41, 1359–1378.

Wang, L., Joshi, S.C., Miller, M.I., Csernansky, J.G., 2001. Statistical analysis of hippocampal asymmetry in schizophrenia. NeuroImage 14, 531–545.

Wang, L., Swank, J.S., Glick, I.E., et al., 2003. Changes in hippocampal volume and shape across time distinguish dementia of the Alzheimer type from healthy aging. NeuroImage 20, 667–682.

Wright, I.C., Rabe-Hesketh, S., Woodruff, P.W., David, A.S., Murray, R.M., Bullmore, E.T., 2000. Meta-analysis of regional brain volumes in schizophrenia. Am. J. Psychiatry 157, 16–25.

Yeterian, E.H., Pandya, D.N., 1988. Corticothalamic connections of paralimbic regions in the rhesus monkey. J. Comp. Neurol. 269, 130–146.

Young, K.A., Manaye, K.F., Liang, C., Hicks, P.B., German, D.C., 2000. Reduced number of mediodorsal and anterior thalamic neurons in schizophrenia. Biol. Psychiatry 47, 944–953.

Zipursky, R.B., Lim, K.O., Sullivan, E.V., Brown, B.W., Pfefferbaum, A., 1992. Widespread cerebral gray volume deficits in schizophrenia. Arch. Gen. Psychiatry 49, 195–205.